5-2015

PDMS microchannel scaffolds for the isolation of individual axon regeneration

Bong Kyun Kim
University of Texas-Pan American

PDMS MICROCHANNEL SCAFFOLDS FOR THE ISOLATION OF INDIVIDUAL AXON REGENERATION

A Thesis

by

BONG KYUN KIM

Submitted to the Graduate School of
The University of Texas-Pan American
In partial fulfillment of the requirement for the degree of

MASTER OF SCIENCE

May 2015

Major Subject: Electrical Engineering

PDMS MICROCHANNEL SCAFFOLDS FOR THE ISOLATION OF INDIVIDUAL AXON REGENERATION

A Thesis
by
BONG KYUN KIM

COMMITTEE MEMBERS

Dr. Yoonsu Choi
Chair of Committee

Dr. Hasina F. Huq
Committee Member

Dr. Daniel Plas
Committee Member

May 2015

ABSTRACT

Bong Kyun Kim, PDMS Microchannel Scaffolds for the Isolation of Individual Axon Regeneration. Master of Science (MS), May, 2015, 27 pp., 15 figures, 37 references, 13 titles.

Injuries to the peripheral nervous system often result in the loss of sensory or motor function within the effected nerve. Nerve scaffolds provide the mechanical support and topographical cues to axon regeneration such that the gap within the injured nerve is bridged and functional recovery is restored. The Microchannel Peripheral Nerve Scaffold, µPNS, was fabricated from PDMS using micromachining techniques that allow for the unprecedented control of microchannel dimensions and paths and therefore, the production of highly customizable Nerve scaffolds for peripheral nerve regeneration applications. The device was then implanted within the sciatic nerves of a series of *Lewis* rats, and was removed after 4 weeks. Each device was then disassembled layer by layer so that every microchannel could be individually inspected. Longitudinal views of axon morphology throughout the length of the scaffolds were collected using three dimensional confocal imaging of the small axon population sample sets, including branching behaviors.

ACKNOWLEDGMENTS

First and foremost, I will always be grateful to Dr.Yoonsu Choi, chair of my thesis committee, for all the mentoring, advice and opportunities he has provided me. I would like to thank Dr. Hasina F. Huq and Dr. Daniel Plas, members of my thesis committee, for their advice and encouragement. I would also like to thank Ridwan Hossain, and Rachel Pankratz for their advice, and suggestions for my thesis. Finally, I would like to express gratitude to J.J. Pickle Research Campus (The University of Texas at Austin), and The University of Texas Health Science Center at San Antonio-Regional Academic Health Center in Edinburg (ERAHC), for all the support they have given my work.

TABLE OF CONTENTS

LIST OF FIGURES

Page

CHAPTER I

INTRODUCTION

The prevalence of peripheral nerve injury within extremities is estimated at from 1.5 to 2.8% and morbidity and low functional recovery are common results [1]. As such, the ultimate goal of nerve conduit design is the restoration of functionality to limbs afflicted by damage to peripheral nerves. After injury, the distal nerve stump begins Wallerian degeneration, in which the myelin sheath and axons start to degenerate, while the proximal stump begins axon degeneration close to the nerve ending [2]. Microphages and monocytes migrate to the endings and remove myelin and axon debris before Schwann cells migrate across the gap to form bands of Bunger from which the extracellular matrix cells begin to regenerate and from which neurotropic factors are produced to facilitate axon growth. At this point Schwann cells begin axon remyelination and axon growth continues until the synaptic target is found and successfully innervated. In instances in which the gap is too long for normal regeneration, axon growth becomes undirected, never reaching the synaptic target, and ceases, in which case the distal end is never reattached and eventually undergoes morbidity [2-4].

A common injury model is a laceration across a peripheral nerve which inhibits the propagation of electrical signals throughout the effected limb. In order to repair the damaged nerve, surgery is required, which includes end-to-end suturing (limited by possible tension on the nerve)[3], and the implantation of autografts, allografts, or nerve conduits of varying design [6]. The most popular clinical approach is the autograft, which requires a second surgical procedure

to remove the donor nerve that results in donor site morbidity [7], and is further complicated by the possibility of dimensional mismatch between the injured and donor nerves. Even when implanted successfully, autografts do not guarantee complete functional restoration, partially due to axons lines within the proximal stump innervating axons within the distal stump of the wrong modality or target muscles. Allografts, like the *Advance*® allograph commercially produced by AxoGen, Inc., remove the difficulties caused by the removal of a donor nerve, but do not support axon growth equal to that of an autograph [8, 9]. Tube conduits fabricated from collagens and various polymers provide some topographical cues and have had limited success restoring functionality, but are often hampered by undirected axon growth within the conduit [10], resulting in modality and target muscle mismatch once again, and nerve constriction which can result in partial nerve morbidity.

Nerve scaffolds, often mimicking the structure of the extracellular scaffold [9, 11-14], provide more topographical cues and increased mechanical support for migrating Schwann cells in comparison with empty tube conduits [10, 15, 16], and can include neurotrophins, like nerve growth factor (NGF), imbedded Schwann cells and stem cells that direct and/or facilitate axon growth [4, 9, 10, 17-21]. Fibrous scaffolds have shown increased directionality by aligning electrospun nanofibers that then give topographical cues for neurites, while some scaffolds have accomplished similar results using topographical cues given by nano-scaled channels or patterns of neurotrophic factors on scaffold surfaces [5, 25-28].

Another approach to increased directionality and regeneration of axons is the inclusion of longitudinal microfluidic channels that induce alignment within a scaffold because they are highly oriented (consequently decreasing improper reinnervation of nerve targets), and provide greater surface area for cell growth [15].

Unfortunately, many microchannel fabrication processes allow very limited manipulation of either channel size, orientation, or position, for instance certain processes that use microwire or fiber channel molds or freeze casting [25, 29, 30]. Examples of extremely precise and uniform microchannel fabrications have be accomplished by either photolithography, the basis of the technique used to fabricate the microchannel peripheral nerve scaffold (μPNS), or by pulsed laser direct write techniques [4, 22, 31, 32].

uPNS have been used to more closely observe neurite regeneration as they, in essence, reduce a nerve segment into a series of axon bundle arrays, and each array provides insight into the regeneration process. The effectiveness of many of these scaffolds are restricted, because process of preparing often destroys the sample. They are also mostly restricted to axon cross sectional views, as longitudinal views risk the integrity of the sample (especially if the microfluidic channels within the sample were not or could not be arranged in a linear uniform manner to horizontal sectioning [5]), and axonal growth patterns are difficult to extrapolate from such fragmented source. None the less, a complete end-to-end views of axon morphology throughout the length of these scaffolds, is a necessary component to understanding the axon regenerative patterns therein. In order to address this issue, a separable layered design was implemented in which each layer only has one flat array of microchannels, as seen in Figure 1.1, and are stacked to form the three dimensional array structure of the scaffold (Figures 1.2). In this way, there is no need to freeze and section the sample, and the entire length of the axon line through the scaffold is available for observation.

Figure 1.1 – Single flat array of microchannel

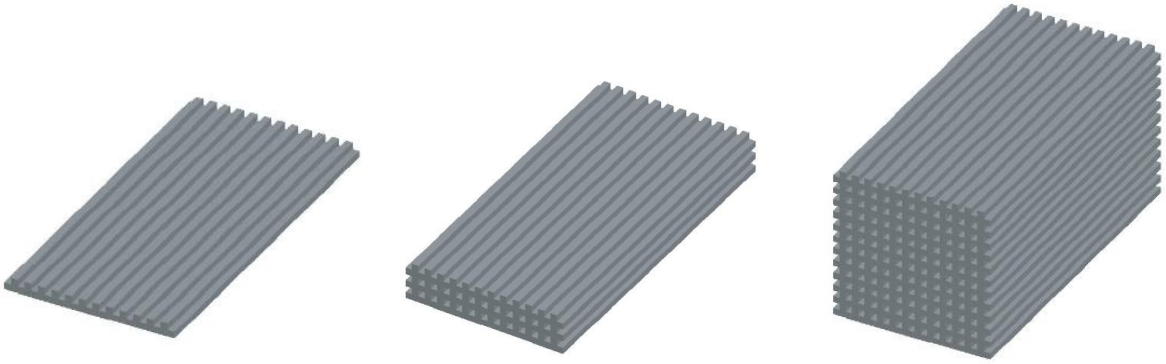

Figure 1.2 – Three dimensional array structure of the scaffold

Observation of axon regeneration is also limited by sample size, as the axons within a longitudinal view often overlap and confuse individual axon paths. By tightly controlling microchannel size, the axon population through it can be controlled, and therefor sample sizes can be restricted.

Scaffolds are commonly fabricated from either polymers or collagens, as polymers, though not usually biodegradable, are biocompatible and collagens are both biocompatible and biodegradable [6, 35]. Polydimethylsiloxane (PDMS), was the preferred material from which to compose µPNS, as it is highly structurally and surface biocompatible, inexpensive, a flexible medium for microfluidic device fabrication like bioassays, has been used in a number of successful

implants such as cochlear implants and pace makers [35], and is sufficiently clear that the individual microchannel layers can be inspected without issue.

CHAPTER II

FABRICATION PROCEDURE

In order to produce the extremely precise PDMS microchannel structures (140um and 40um microchannel) that comprise the µPNS, a master structure mold first needed to be fabricated using the photolithographic procedure seen in Figure 2.1.

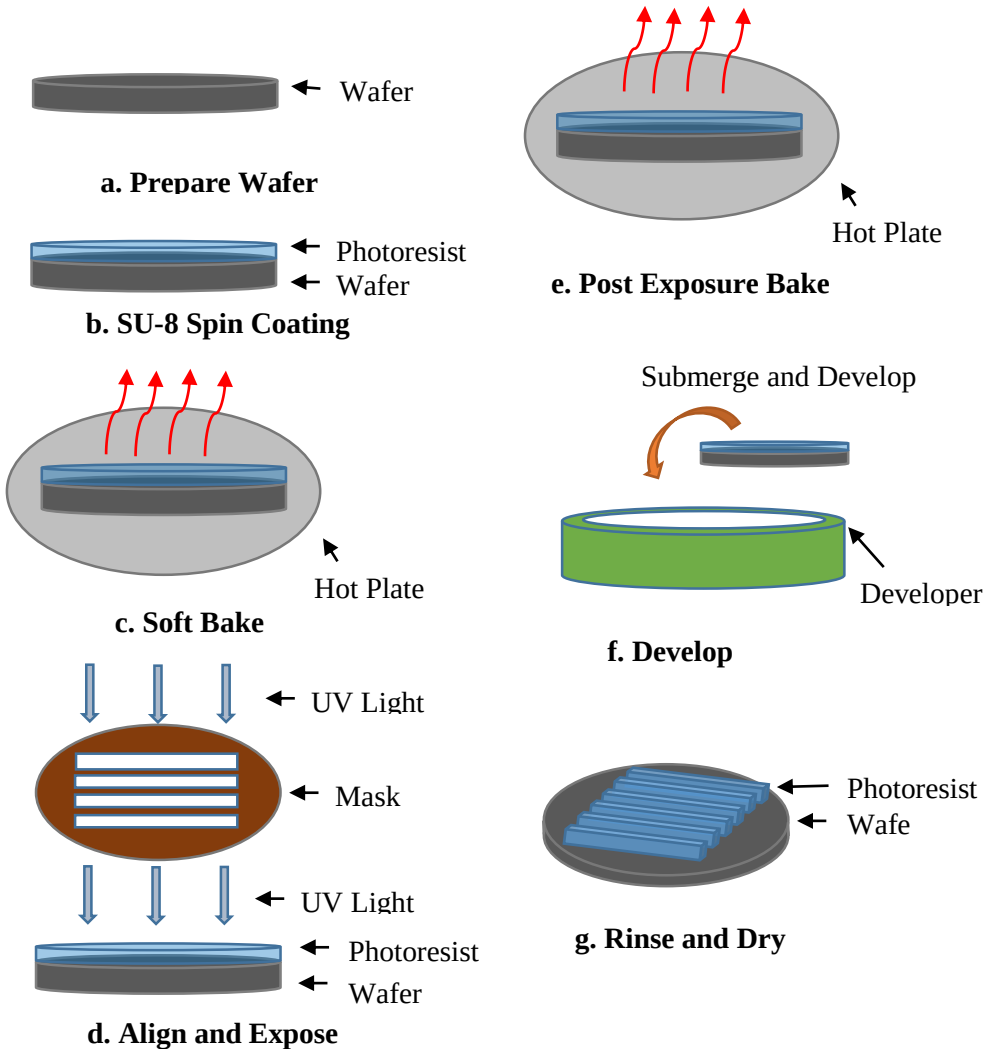

Figure 2.1 – Master structure fabrication

2.1 Master Structure Fabrication

A three inch diameter silicon wafer was first sprayed with isopropyl alcohol, dried with a nitrogen gun, and placed on a hotplate to prepare and clean the surface prior to the application of the photoresist and placed in the spinning machine. Two thirds of the wafer was covered by the SU-8 2035 photoresist. The wafer was then spin-coated 900rpm for 30seconds for 140um sample, and 3250rpm for 30seconds for 40um sample. The sample was then placed on a level hotplate at 95℃ for 20minutes for 140um sample, and 6minutes for 40um sample.

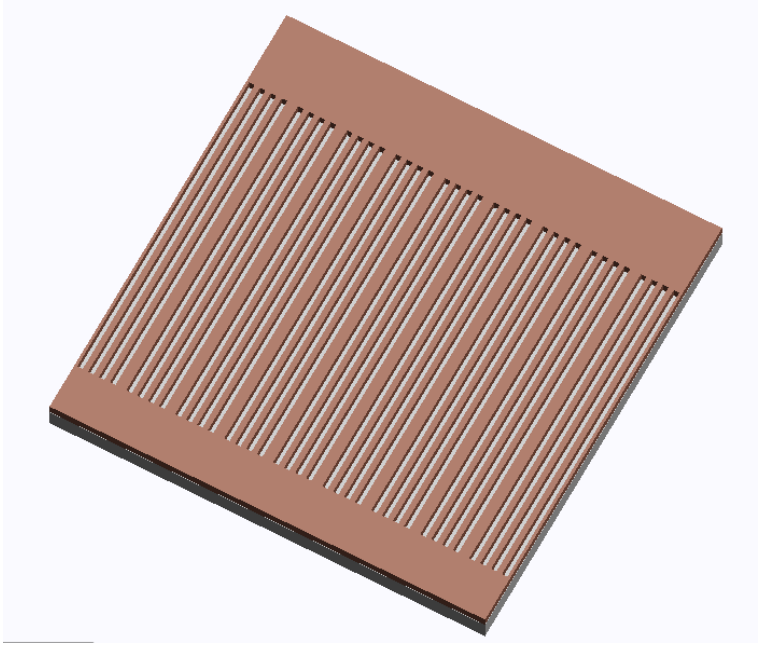

Figure 2.2 – Microchannel pattern mask

In order to fabricate the channel pattern seen in Figure 2.2, a mask pattern was first designed in AutoCAD, then the channel patterned film was placed on a four inch glass plate coated with chromium and AZ1518 photoresist (Figure 2.3), placed on the MJB4 Suss Microtec® mask aligner, and then exposed to UV light.

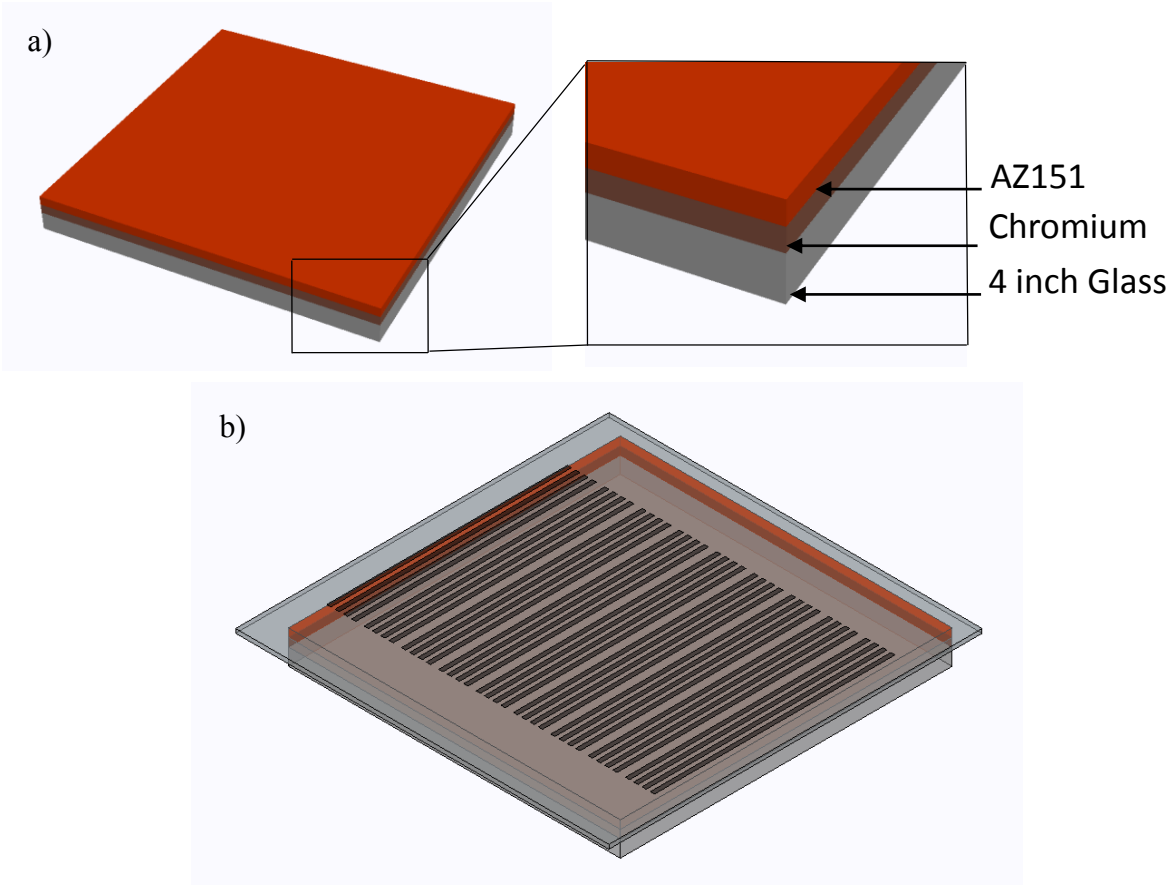

Figure 2.3 – a) Chromium glass b) Chromium glass with film

After exposure, the sample was placed in 400K developer solution for two and a half minutes, rinsed in deionized water and dried with a nitrogen gun. The sample was then placed in a chromium etchant for three minutes, rinsed with deionized water and dried with a nitrogen gun. Lastly the sample was washed with acetone and rinsed with deionized water to remove remaining AZ1518 photoresist and form the chrome mask (Figure 2.2, and 2.4c).

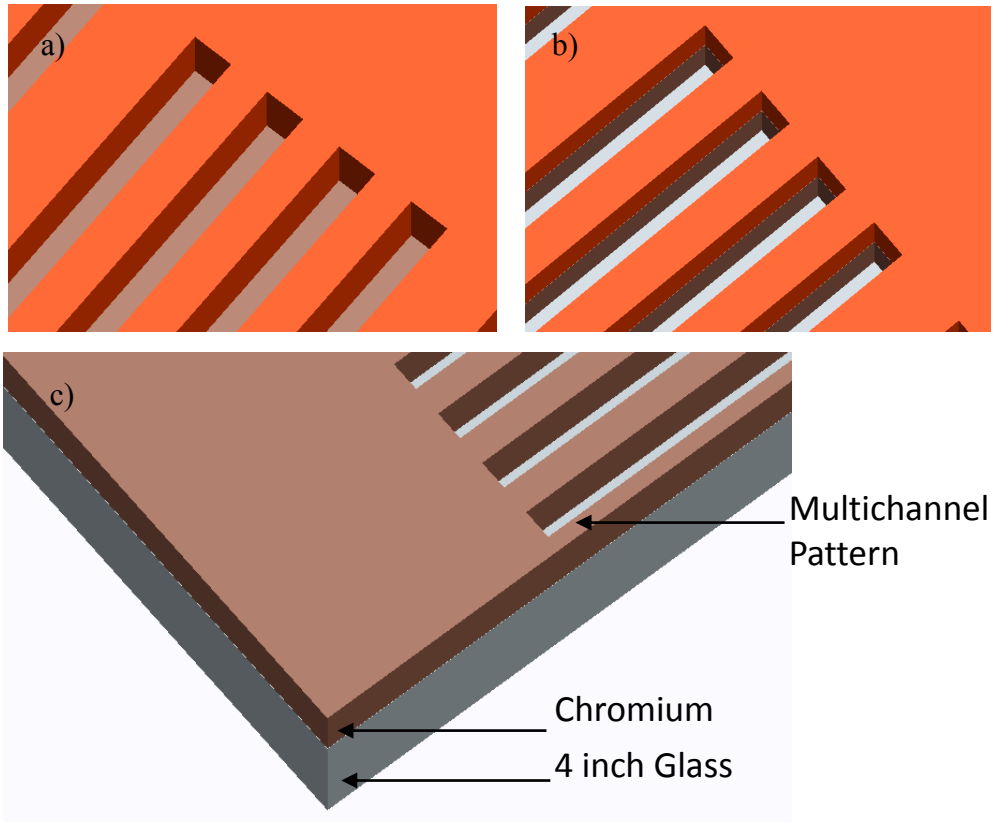

Figure 2.4 – Chromium glass a) after develop b) after etch c) after washed with acetone

The SU-8 covered silicon wafer was placed on the mask aligner with the chromium glass mask on top of it, aligned and then exposed to UV light with light intensity of 250mJ/cm^2 for 140um sample and 160mJ/cm^2 for 40um sample. Immediately after exposure, the silicon wafer was placed on the hotplate at 95℃ for 10minutes for 140um sample and 5minutes for 40um sample, and removed to cool. The post exposure bake solidify the photoresist to a permanent structure. The sample was then placed in SU-8 developer for 12minutes for 140um sample and 5minutes for 40um sample to remove the unexposed portion of the photoresist. At this point, the

master structure mold is complete, and the microchannel patter can be seen. (Figure 2.5) The master structure was then rinsed with deionized water and dried with a nitrogen gun.

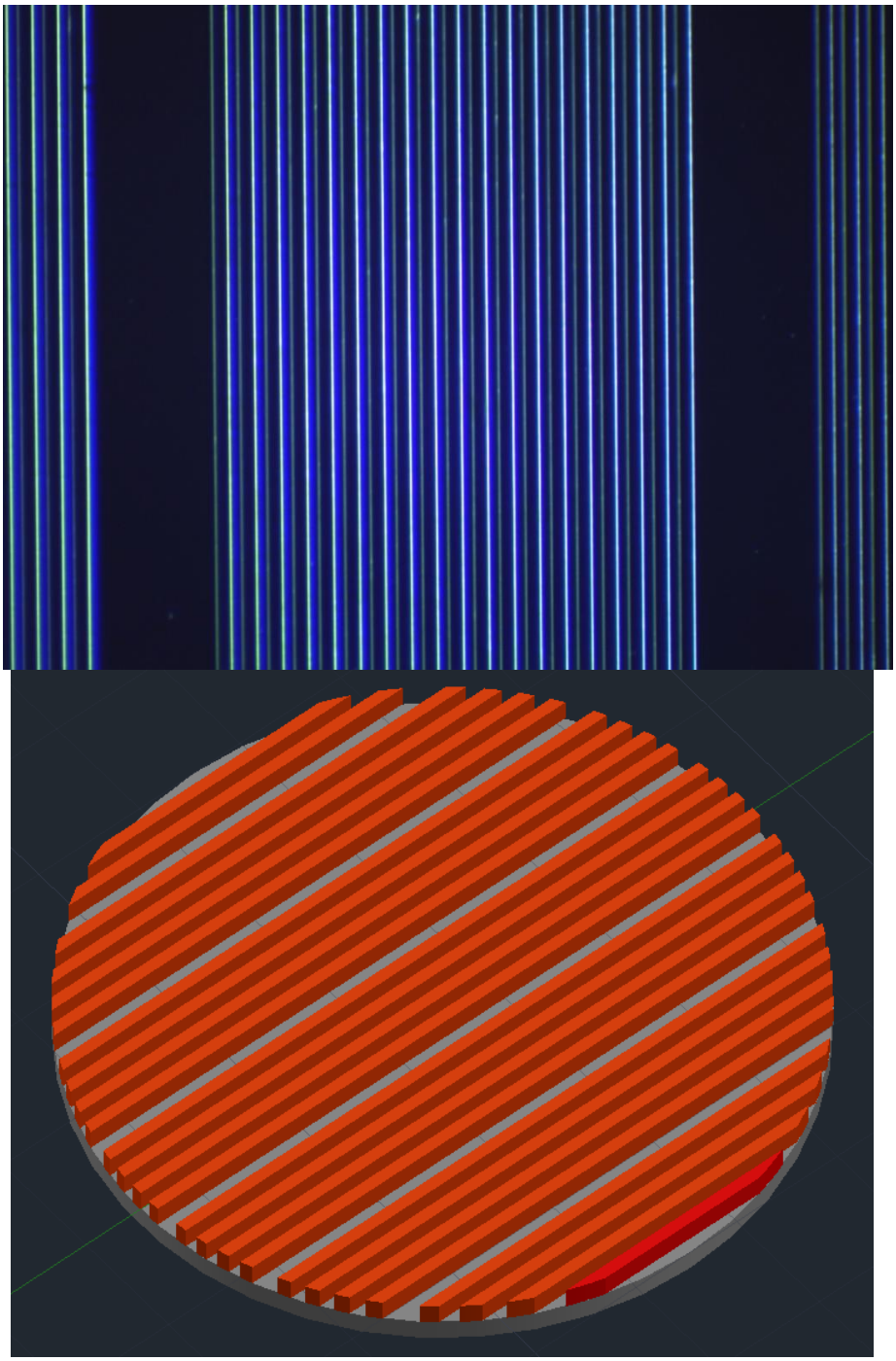

Figure 2.5 – Master structure on silicon wafer

2.2 PDMS Microchannel Layer Fabrication

Master structure was covered by the 10:1 PDMS mixture (Sylgard® 184, Dow Corning® , MI) then spin-coated for 800rpm for 30seconds for 140um sample, and 3000rpm for 30seconds for 40um sample. This was then cured in an oven for 30minutes at 95℃, removed and allowed to cool. The structure was then submerged in a chloroform solution, within which the PDMS solution expanded and detached from the SU-8 master structure. The PDMS layer was then submerged in an isopropyl alcohol solution until it retracted to its original size and simultaneously removed any chloroform remaining on it, removed from the solution, and allowed to air dry.

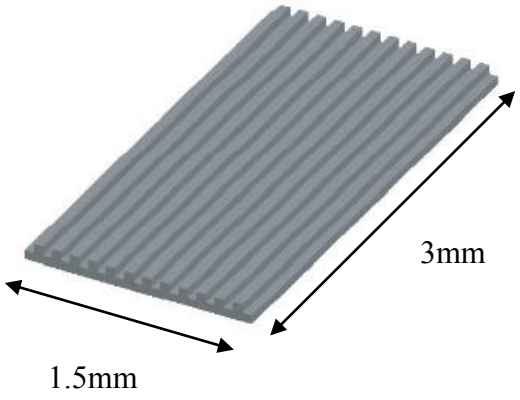

Figure 2.6 – Single PDMS layer

At this juncture, the PDMS structure is sectioned into a series of appropriately dimensioned multichannel layers with a sharp blade, as seen in Figure 2.6. PDMS thin film was layered on a glass plate and cut into a 2 cm by 7 mm rectangle, and a single microchannel layer was bonded with 10:1 PDMS to curing agent mixture (Sylgard® 186, Dow Corning® , MI) to the thin film, as seen in Figure 2.7b. After the PDMS cured, microchannel layers were stacked to approximately 1.5 mm so that the structure cross-section is approximately square (Figure 2.8). The thin film was wrapped around the microchannel scaffold structure twice, and 10:1 PDMS to curing agent

mixture (Sylgard® 186, Dow Corning®, MI) was applied to the thin film, securing the microchannel layers together into a cohesive structure (Figures 2.7e, 2.7f, 2.8, and 2.9).

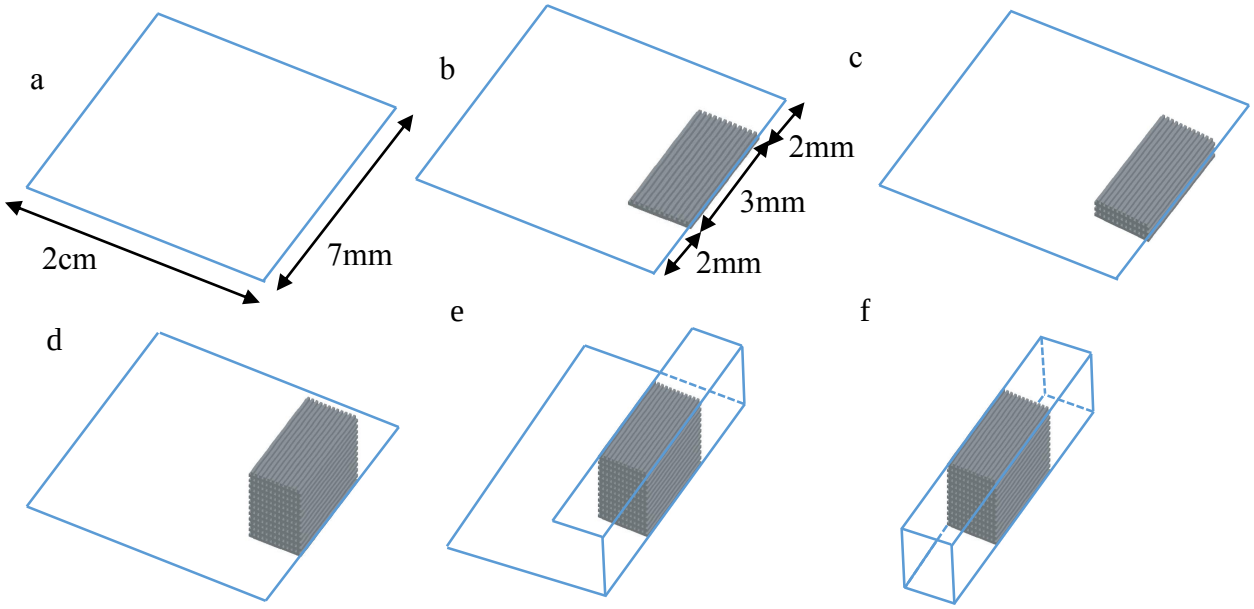

Figure 2.7 – PDMS microchannel layer fabrication

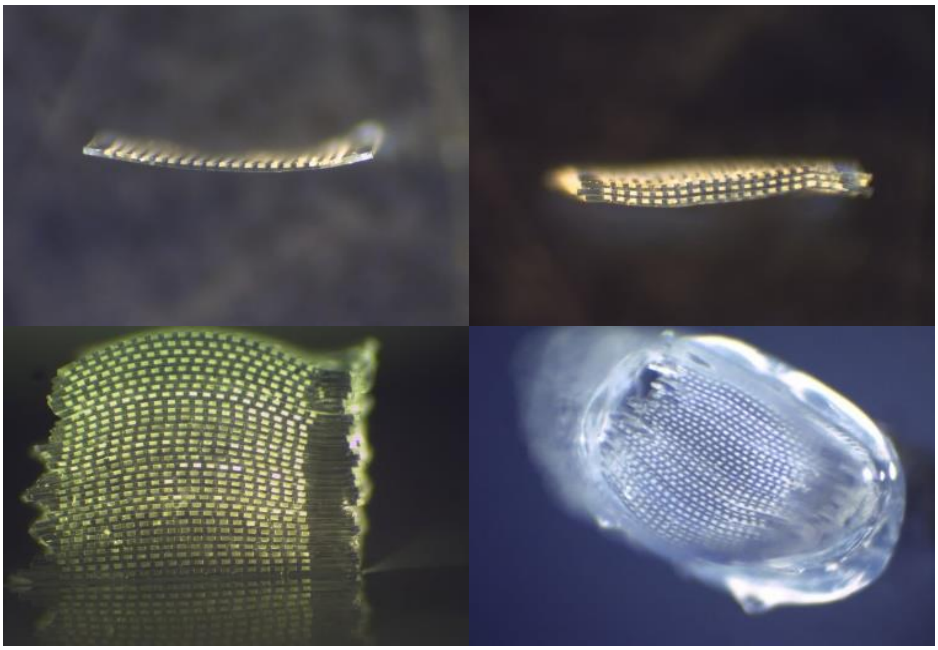

Figure 2.8 – Cross section of PDMS layers

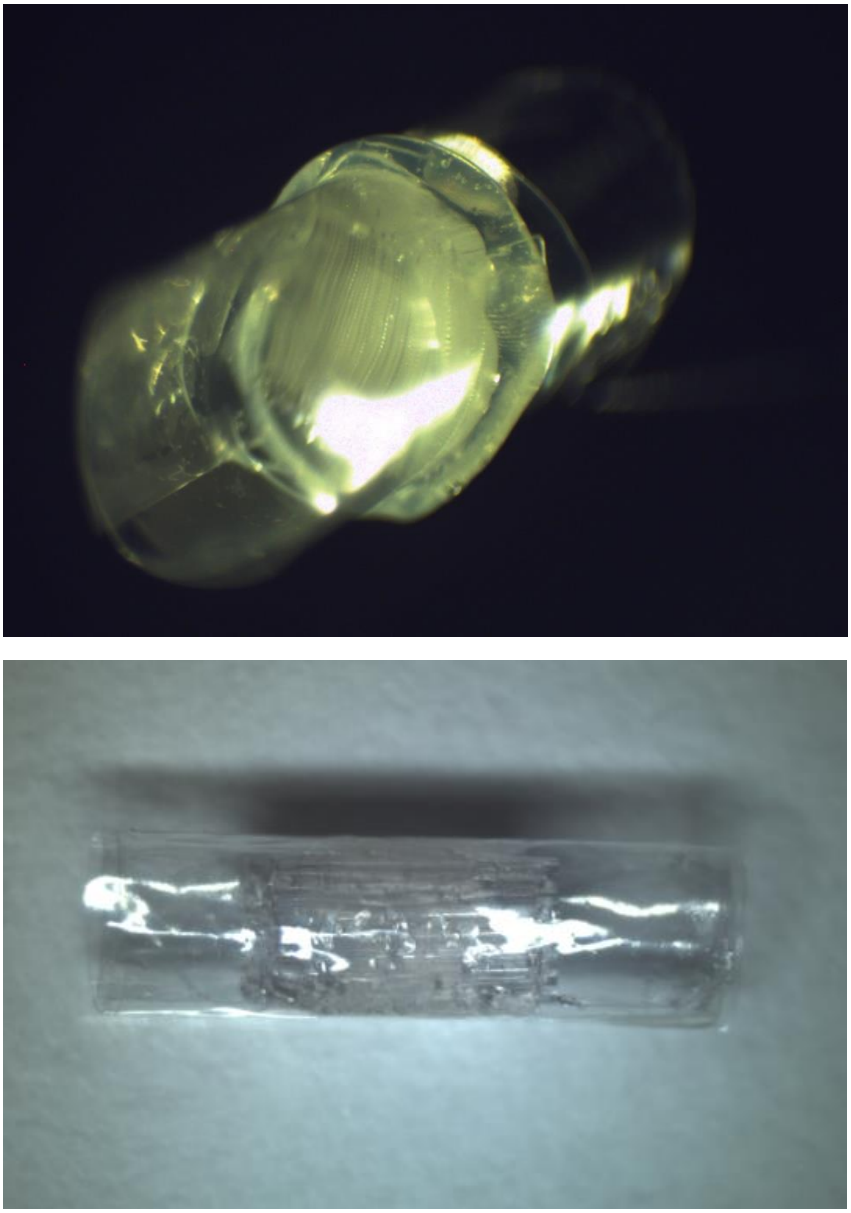

Figure 2.9 – PDMS microchannel scaffold

CHAPTER III

SURGICAL PROCEDURE

Surgical procedures were performed under aseptic conditions at the UTPA Animal Facility. Prior to implantation, a *Lewis* rat was placed into an induction chamber and subjected to gas anaesthesia (Isoflurane) until unconscious. The surgery location (right thigh) was shaved and cleaned using a betadine scrub and isopropyl alcohol. Its maxillary central incisors were hooked into a gas mask through which it continued to receive small doses of anaesthesia. It was secured to a surgery table and its body temperature was regulated with the placement of a heat pad. Incisions were made along the right thigh to expose the sciatic nerve. The nerve was severed, proximal to the tibial and fibular nerves, and a μPNI was implanted by suturing both the distal and proximal ends of the nerves to the guides of the device. All procedures conformed to the Guide for the Care and Use of Laboratory Animals of the Institute of Laboratory Animal Resources, Commission on Life Sciences, National Research Council[41]. They were reviewed and approved by the Institutional Animal Care and Use Committee UTPA.

CHAPTER IV

HISTOLOGY

Four weeks after device implantation, animals were euthanized and perfused through the heart with saline followed by 4% paraformaldehyde. The integrity of the regenerated sciatic nerve was examined and post-fixed for 24 hours in 4% paraformaldehyde (Sigma-Aldrich). The samples were rinsed again in PBS and transferred to 30% sucrose solution in phosphate buffer, pH 7.4, for cryoprotection. Figure 4.1 shows the harvested tissue at the current step in which white coloured regenerated nerve and the microchannel scaffold are observed together.

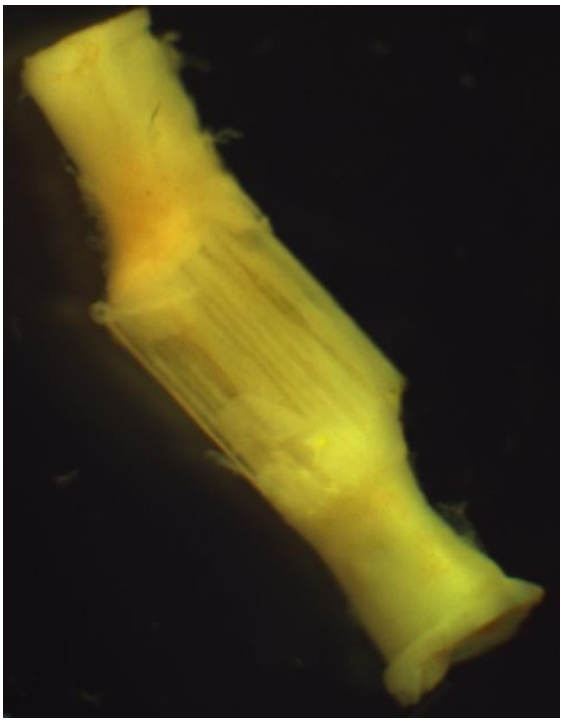

Figure 4.1 – Harvested tissue with microchannel scaffold

The samples were then embedded in O.C.T. gel (Tissue Tek) and stored at -80℃ until the time of cryosectioning. A cryostat (CM30505, Leica) was used to collect cross-sectional nerve tissues from proximal side. When it reached the end of the microchannel scaffold, cryosectioning was stopped. OCT around the sample was melted down to extract the microchannel scaffold. Individual layers can be separated as no adhesive was used between the layers.

Sections were later reacted for immunofluorescent demonstration of markers on axons (NF160, 1:250 dilution, Sigma–Aldrich). Nuclei were labelled with DAPI (Invitrogen). Goat anti-mouse IgG1 Alexa 488 was used as a secondary antibody. After cleaning OCT, tissue sections were first incubated for one hour at room temperature in a blocking solution of 4% goat serum (Gibco) in PBS containing 0.5% Triton X-100 (Sigma). Sections were then incubated overnight at 4 ℃ in a mixture of primary antibody and blocking solution, then washed and incubated once more for 1 hour at room temperature in a solution of secondary antibody, diluted 1:220 in 0.5% Triton in PBS. Finally, the sections were washed once more and dried. Mounting media (Fluoromount-G™ with DAPI, eBioscience) was applied on the tissue and cover-slipped for evaluation. Sections were imaged using a confocal microscope (Olympus FV10i).

CHAPTER V

RESULT

The precise control over the fabrication of the microchannel layers allowed for extremely small microchannels dimensions that could restrict axon regeneration to four or less axon lines through every channel. To highlight this, two Nerve scaffolds were fabricated with 140µm and 40µm channel widths respectively, implanted within the sciatic nerves of a series of *Lewis* rats, were removed after four weeks, and then compared for axon population using IHC analysis (in which individual layers were stained with NF160).

Figure 4.1, and Figure 4.2 shows the actual channel width comparisons, and, as can be seen in Figures 4.2, that the decreased channel size successfully reduced the axon population. IHC analysis for the 140um channel scaffold shows twenty five to thirty five axons per microchannel when inspected using a confocal microscope (Olympus FV 1000). Though axon growth through the 140 µm channels successfully bridged the nerve gap, the convoluted and overlapping images of axon morphology made the study of individual axon growth patterns are challenge. IHC analysis for the 40um channel scaffold shows one to four axons per microchannel when inspected using a confocal microscope (Olympus FV 1000). The confocal microscope images were processed using FV10-ASW 3.1 software's Z-stack function at different depths (29 steps, 34.16um height) for the three dimensional figures, and the "Intensity projection over z axis" function was use to combine z stack pictures to observe axon lines clearly for the two dimensional figures.

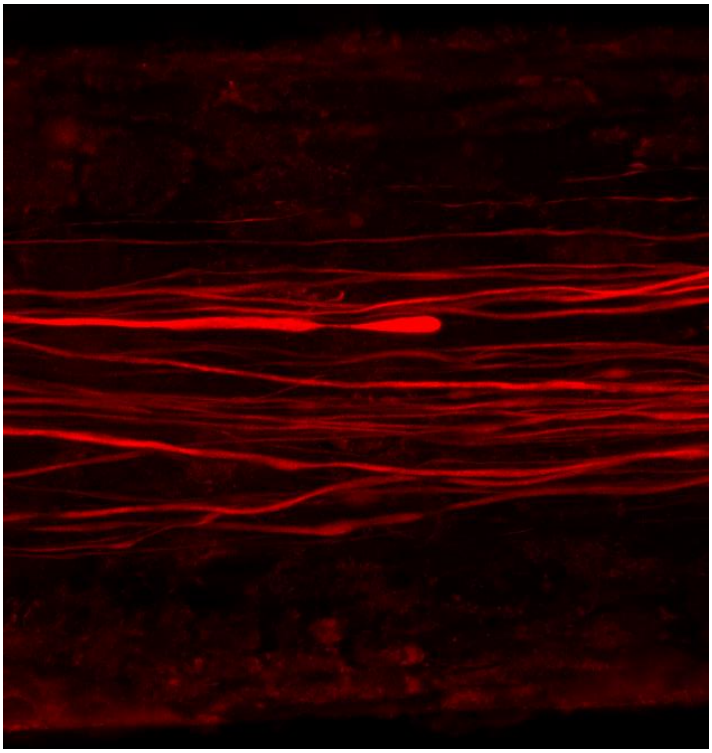

Figure 4.1 – Axon population of 140um microchannel

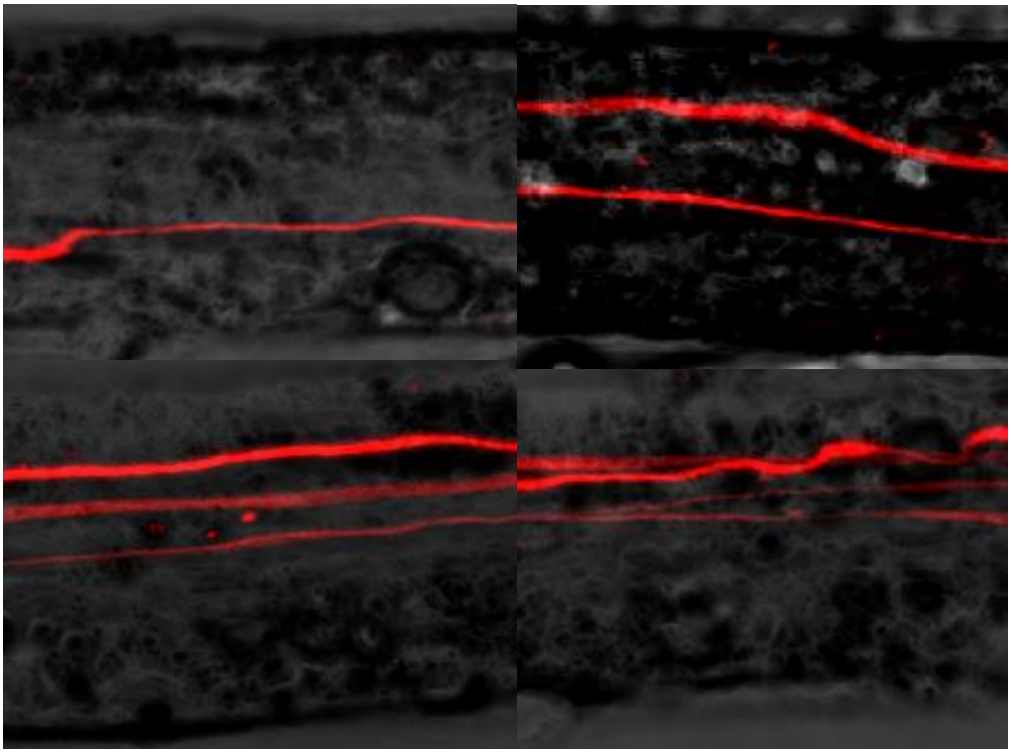

Figure 4.2 – Axon population of 40um microchannel

Figures 4.3 contains three dimensional rendered confocal image examples of each of the regrowth possibilities for a 40µm channel, with Figure 4.3D presenting a case of axon branching.

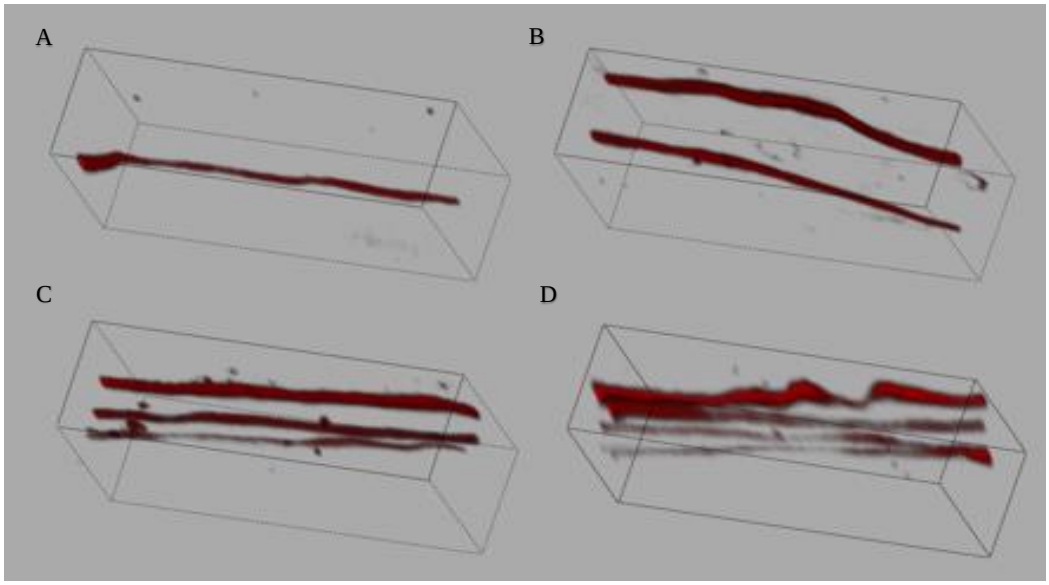

Figure 4.3 – Three dimensional rendering of axon population (single, two, three and four axons per 40um microchannel)

CHAPTER VI

FUTURE DIRECTIONS

The results presented in the previous section is an indication of the possible discoveries pertaining to axon regeneration that would be previously unobservable due to a combination of cross-section restricted views and overlapping axon lines. In combination with neuron growth factor or other neurotrophins, a subject of future studies using this scaffold design, the µPNS could have an even greater potential for axon regeneration and provide a greater insight to their effect on the regeneration process. µPNS not only provides a highly customizable platform for Nerve scaffolds production, it also provides a platform from which the effect of current research interests and treatments on axon morphology can be more thoroughly scrutinized and better understood, such as electrical stimulation post implantation [36, 37] or the addition of Schwann cells [20], neurotrophic factors [6], or stems cells [9] within Nerve scaffolds structures.

Though single axon morphology observation is an important step in understanding axon regeneration, its most interesting possible application is as a base for a three dimensional nerve interface. Most electrode interfaces are divided in to three categories: cuff, penetrating, and regenerative electrodes [34]. Cuff electrodes encircle the entire nerve outside the epineurium and innervate the entire nerve, and, as such, are not adequately selective for some prosthetic and other applications which require innervation of axons with a specific target [34] as, even within a specific fascicle, axons can have differing or even multiple target muscles. Penetrating electrodes are more selective, capable of recording or innervating a fascicle, but are unable to selectively access a

single axon line. They also are prone to signal degradation as implant movement within the nerve eventually leads to scarring around the probe [33, 34]. Regenerative electrodes have the highest amount of selectivity but are also the most invasive type of electrode. Scaffold's length, and diameter for microchannel can be controlled and accessing small groups of axons are possible [5]. For long term applications, regenerative electrodes have had some success, though the issue of axon selectivity remains [33, 34], therefore the addition of a long term electrode array embedded within a nerve scaffold capable of selectively innervating or recording from a single or a small population of axons, may present the best approach for nerve interface design.

Because a photolithographic process is used to fabricate the μPNS, the addition of electrical lines and contact pads are easily included with minimal changes to the overall design of the scaffold. Electrodes can be included within all the microchannels within a PDMS layer, and many electrode PDMS layers can be included within a single implant forming a multilayer electrode array in which every electrode can be selectively accessed.

CHAPTER VII

CONCLUSION

A PDMS based microchannel nerve scaffolds was designed, with the ability to be disassembled post implantation without sectioning, which could isolate axon populations within a channel to one to four axons, such that individual axon morphologies could be observed. The microchannel scaffold was then implanted in the sciatic nerve of *Lewis* rats, removed after four weeks, and studied under a confocal microscope. Two sets of microchannel scaffolds were implanted, one composed of 140µm in width, and the other composed of 40 µm in width, to confirm that axon population and microchannel width have a directly proportional relationship. The 40 µm channel scaffolds consistently showed axon regrowth through the length of the channels, and restricted the axon populations within channels to four or less.

One of the most promising aspect of this design is its capability to be adapted for nerve interface applications where electrical signals from single axons are required to be recorded or modified. Because of µPNS's photolithographic fabrication process, the simple inclusion of metal contacts and electrical lines could be added onto PDMS layers with relative ease and minimal changes to the scaffold structure.

REFERENCES

[1] S. Yegiyants, "Traumatic Peripheral Nerve Injury: A Wartime Review," Journal of Craniofacial Surgery, vol. 21, pp. 998-1001, 2010.

[2] R. Siddique and N. Thakor, "Investigation of nerve injury through microfluidic devices," Journal of the Royal Scociety Interface, vol. 11, pp. 1-13, 2014.

[3] X. Gu, F. Ding, and D. F. Williams, "Neural tissue engineering options for peripheral nerve regeneration," Biomaterials, vol. 35, pp. 6143-6156, 2014.

[4] A. Rajaram, X.-B. Chen, and D. J. Schreyer, "Strategic design and recent fabrication techniques for bioengineered tissue scaffolds to improve peripheral nerve regeneration," Tissue Engineering: Part B, vol. 18, pp. 454-467, 2012.

[5] Kim, Bongkyun, Alejandro Reyes, Bernardo Garza, and Yoonsu Choi. "A microchannel neural interface with embedded microwires targeting the peripheral nervous system." *Microsystem Technologies* (2014): 1-7.

[6] W. Daly, L. Yao, D. Zeugolis, A. Windebank, and A. Pandit, "A biomaterials approach to peripheral nerve regeneration: bridging the peripheral nerve gap and enhancing functional recovery," Journal of the Royal Scociety Interface, vol. 9, pp. 202-221, 2012.

[7] K. E. Tansey, J. L. Seifert, B. Botterman, M. R. Delgado, and M. I. Romero, "Peripheral Nerve Repair Through Multi-Luminal Biosynthetic Implants," Annals of Biomedical Engineering, vol. 39, pp. 1815-1828, 2011.

[8] E. C. Spivey, Z. Z. Khaing, J. B. Shear, and C. E. Schmidt, "The fundamental role of subcellular topography in peripheral nerve repair therapies," Biomaterials, vol. 33, pp. 4264-4276, 2012.

[9] Y. Zhang, H. Luo, Z. Zhang, Y. Lu, X. Huang, L. Yang, et al., "A nerve graft constructed with xenogeneic acellular nerve matrix and autologous adipose-derived mesenchymal stem cells," Biomaterials vol. 31, pp. 5312-5324, 2010.

[10] J. Cao, C. Sun, H. Zhao, Z. Xiao, B. Chen, J. Gao, et al., "The use of laminin modified linear ordered collagen scaffolds loaded with laminin-binding ciliary neurotrophic factor for sciatic nerve regeneration in rats " Biomaterials, vol. 32, pp. 3939-3948, 2011.

[11] X. Hu, J. Huang, Z. Ye, L. Xia, M. Li, B. Lv, et al., "A novel scaffold with longitudinally oriented microchannels promotes peripheral nerve regeneration," Tissue Engineering Part A, vol. 15, pp. 3297-3308, 2009.

[12] A. Bozkurt, F. Lassner, D. O'Dey, R. Deumens, A. Böcker, T. Schwendt, et al., "The role of microstructured and interconnected pore channels in a collagen-based nerve guide on axonal regeneration in peripheral nerves," Biomaterials, vol. 33, 2012.

[13] P. X. Ma, "Biomimetic materials for tissue engineering," Advanced Drug Delivery Reviews, vol. 60, pp. 184-198, 2008.

[14] S. Gao, Y. Zheng, Q. Cai, W. Yao, J. Wang, P. Zhang, et al., "Comparison of morphology and biocompatibility of acellular nerve scaffolds processed by different chemical methods," Journal of Material Science: Materials in Medicine, vol. 25, pp. 1283-1291, 2014.

[15] R. T. Tran, W. M. Choy, H. Cao, I. Qattan, J.-C. Chiao, W. Y. Ip, et al., "Fabrication and characterization of biomimetic multichanneled crosslinked-urethane-doped polyester tissue engineered nerve guides," Journal of Biomedical Materials Research Part A, vol. 102, pp. 2793-2804, 2014.

[16] Q. Fu, M. N. Rahaman, S. Bal, K. Kuroki, and R. F. Brown, "In vivo evaluation of 13-93 bioactive glass scaffolds with trabecular and oriented microstructures in a subcutaneous rat implantation model," Journal of Biomedical Materials Research Part A, vol. 95, pp. 235-244, 2010.

[17] K. Krick, M. Tammia, R. Martin, A. Hoke, and H.-Q. Mao, "Signaling cue presentation and cell delivery to promote nerve regeneration," Current Opinion in Biotechnology, vol. 22, pp. 741-746, 2011.

[18] H. Xia, Q. Chen, Y. Fang, D. Liu, D. Zhong, H. Wu, et al., "Directed neurite growth of rat dorsal root ganglion neurons and increased colocalization with Schwann cells on aligned poly(methyl methacrylate) electrospun nanofibers," Brain Research, vol. 1565, pp. 18-27, 2014.

[19] T. Führmann, L. M. Hillen, K. Montzka, M. Wöltje, and G. A. Brook, "Cell-Cell interactions of human neural progenitor-derived astrocytes within a microstructured 3D-scaffold," Biomaterials, vol. 31 pp. 7705-7715, 2010.

[20] A. Bozkurt, R. Deumens, C. Beckmann, L. O. Damink, F. Schugner, I. Heschel, et al., "In vitro cell alignment obtained with a Schwann cell enriched microstructured nerve guide with longitudinal guidance channels," Biomaterials, vol. 30, pp. 169-179, 2008.

[21] W. Zeng, M. Rong, X. Hu, W. Xiao, F. Qi, J. Huang, et al., "Incorporation of Chitosan Microspheres into Collagen Chitosan Scaffolds for the Controlled Release of Nerve Growth Factor," PLOS ONE, vol. 9, pp. 1-9, 2014.

[22] O. Sarig-Nadir, N. Livnat, R. Zajdman, S. Shoham, and D. Seliktar, "Laser photoablation of guidance microchannels into hydrogels directs cell growth in three dimensions," Biophysical Journal, vol. 93, pp. 4743-4752, 2009.

[23] D. Lynam, C. Peterson, R. Maloney, D. Shahriari, A. Garrison, S. Saleh, et al., "Augmenting protein release from layer-by-layer functionalized agarose hydrogels," Carbohydrate Polymers, vol. 103, pp. 377-384, 2014.

[24] D. Lynam, "Multifunctional Hydrogel Nerve Guidance Scaffolds for Central and Peripheral Nerve Repair," Doctor of Philosophy, Materials Science and Engineering, Michigan State University, Ann Arbor, MI, 2014.

[25] D. Lynam, B. Bednark, C. Peterson, D. Welker, M. Gao, and J. S. Sakamoto, "Precision microchannel scaffolds for central and peripheral nervous system repair," Journal of Material Science: Materials in Medicine, vol. 22, pp. 2119-2130, 2011.

[26] V. Mukhatyar, B. Pai, I. Clements, A. Srinivasan, R. Huber, A. Mehta, et al., "Molecular Sequelae of Topographically Guided Peripheral Nerve Repair," Annals of Biomedical Engineering, vol. 42, pp. 1436-1455, 2013.

[27] L. Yao, S. Wang, W. Cui, R. Sherlock, C. O'Connell, G. Damodaran, et al., "Effect of functionalized micropatterned PLGA on guided neurite growth," Acta Biomaterialia, vol. 5, pp. 580-588, 2009.

[28] H. N. Kim, A. Jiao, N. S. Hwang, M. S. Kim, D. H. Kang, D.-H. Kim, et al., "Nanotopography-guided tissue engineering and regenerative medicine," Advanced Drug Delivery Reviews, vol. 65, pp. 536–558, 2013.

[29] K. Uto, T. Muroya, M. Okamoto, H. Tanaka, T. Murase, M. Ebara, et al., "Design of super-elastic biodegradable scaffolds with longitudinally oriented microchannels and optimization of the channel size for Schwann cell migration," Science and Technology of Advanced Materials, vol. 13, pp. 1-10, 2012.

[30] A. Saglam, A. Perets, A. C. Canver, H.-L. Li, K. Kollins, G. Cohen, et al., "Angioneural Crosstalk in Scaffolds with Oriented Microchannels for Regenerative Spinal Cord Injury Repair," Journal of Molecular Neuroscience, vol. 49, pp. 334-346, 2013.

[31] A. Srinivasan, M. Tahilramani, J. T. Bentley, R. K. Gore, D. C. Millard, V. J. Mukhatyar, et al., "Microchannel-based regenerative scaffold for chronic peripheral nerve interfacing in amputees," Biomaterials, vol. 41, pp. 151-165, 2015.

[32] A. Srinivasan, L. Guo, and R. V. Bellamkonda, "Regenerative Microchannel Electrode Array for Peripheral Nerve Interfacing," in 5th International IEEE EMBS Conference on Neural Engineering, Cancun, Mexico, 2011.

[33] P. A. Wieringa, R. W. F. Wiertz, E. L. d. Weerd, and W. L. C. Rutten, "In vitro Verification of a 3-D Regenerative Neural Interface Design: Examination of Neurite Growth and Electrical Properties Within a Bifurcating Microchannel Structure " Proceedings of the IEEE, vol. 98, pp. 389-397, 2010.

[34] I. I. Stoyanova, R. J. A. v. Wezel, and W. L. C. Rutten, "In vivo testing of a 3D bifurcating microchannel scaffold inducing separation of regenerating axon bundles in peripheral nerves," Journal of Neural Engineering, vol. 10, pp. 1-13, 2013.

[35] C. Hassler, T. Boretius, and T. Stieglitz, "Polymers for Neural Implants," Journal of Polymer Science: Part B: Polymer Physics, vol. 49, pp. 18-33, 2011.

[36] J. Huang, L. Lu, X. Hu, Z. Ye, Y. Peng, X. Yan, et al., "Electrical stimulation accelerates motor functional recovery in the rat model of 15-mm sciatic nerve gap bridged by scaffolds with longitudinally oriented microchannels," Neurorehabilitation and Neural Repair, vol. 24, pp. 736-745, 2010.

[37] K. Haastert-Talini, R. Schmitte, N. Korte, D. Klode, A. Ratzka, and C. Grothe, "Electrical stimulation accelerates axonal and functional peripheral nerve regeneration across long gaps," Journal of Neurotrauma, vol. 28, pp. 661-674, 2011.

BIOGRAPHICAL SKETCH

Bong Kyun Kim was born in Seoul, South Korea in 1987. The majority of his life was spent growing up in New Jersey and Pennsylvania, developing a fascination for technology and engineering. Bong Kyun received his Bachelor's degree from the Pennsylvania State University in 2013 and his Master's degree from the University of Texas-Pan American in 2015. While pursuing his Master degree, he has presented research in Neural Interfaces Conference, Biomedical Engineering Society, IEEE Industrial Electronics Society, and Neuroscience. Additionally he has published his research in the journal, Microsystem Technologies. His main research interests are peripheral neural interface and he maintained a 4.0 average throughout his graduate career and his conducted research includes fabricating micro peripheral nerve scaffold and ECoG by using micromachining technology at J.J. Pickle Research Campus (University of Texas at Austin). Upon graduation from the University of Texas-Pan American, Bong Kyun is looking forward to beginning PhD program in the United States.

Permanent address: Xii Harborview Apt 101Dong 2001Ho Songdo-Dong Yeonsu-Gu Incheon
406-840 South Korea

Permanent email address: vision0752@gmail.com